(14) WRE-TR-1907(A)

AR-000-973

DEPARTMENT OF DEFENCE

DEFENCE SCIENCE AND TECHNOLOGY ORGANISATION

WEAPONS RESEARCH ESTABLISHMENT

SALISBURY, SOUTH AUSTRALIA

(9) TECHNICAL REPORT 1907 (A)

(6) METEOROLOGICAL AND GROUND EFFECTS ON THE PROPAGATION OF AIRCRAFT NOISE CLOSE TO THE EARTH'S SURFACE.

(10) C.J. CHESSELL

(12) 30 p.

Approved for public release

(C) Commonwealth of Australia

(11) DECEMBER 1977

AR-000-973

DEPARTMENT OF DEFENCE

DEFENCE SCIENCE AND TECHNOLOGY ORGANISATION

WEAPONS RESEARCH ESTABLISHMENT

TECHNICAL REPORT 1907 (A)

METEOROLOGICAL AND GROUND EFFECTS ON THE PROPAGATION OF AIRCRAFT NOISE CLOSE TO THE EARTH's SURFACE

C.I. Chessell

ABSTRACT

SUMMARY

Dickinson (J. Sound and Vib 47, 438-443, 1976) reported observations of unexpectedly low attenuations between aircraft take-off noise levels measured at ranges of 320 m and 2900 m at London (Gatwick) Airport. The anomalous attenuations were attributed to the effects of focussing by a temperature inversion. These data are investigated and a ray trace study shows that the low attenuations are unlikely to be caused by atmospheric focussing by the temperature inversion. Further, it is shown that a combination of the effects of a finite impedance ground and of atmospheric refraction in overcoming part of the ground absorption at the distant position can adequately explain the observed data.

ABSTRACT

Approved for Public Release

POSTAL ADDRESS: The Director, Weapons Research Establishment,
Box 2151, G.P.O., Adelaide, South Australia, 5001.

DOCUMENT CONTROL DATA SHEET

Security classification of this page: UNCLASSIFIED

1 DOCUMENT NUMBERS	2 SECURITY CLASSIFICATION
AR Number: AR-000-973	a. Complete Document: Unclassified
Report Number: WRE-TR-1907 (A)	b. Title in Isolation: Unclassified
Other Numbers:	c. Summary in Isolation: Unclassified

3 TITLE: METEOROLOGICAL AND GROUND EFFECTS ON THE PROPAGATION OF AIRCRAFT NOISE CLOSE TO THE EARTH'S SURFACE

4 PERSONAL AUTHOR(S):	5 DOCUMENT DATE:
C.I. Chessell	December 1977
	6 6.1 TOTAL NUMBER OF PAGES 28
	6.2 NUMBER OF REFERENCES: 11

7 7.1 CORPORATE AUTHOR(S):	8 REFERENCE NUMBERS
Weapons Research Establishment	a. Task: AUS 75/44
7.2 DOCUMENT (WING) SERIES AND NUMBER TR-1907 Applied Physics Wing	b. Sponsoring Agency:
	9 COST CODE: 130922

10 IMPRINT (Publishing establishment):	11 COMPUTER PROGRAM(S) (Title(s) and language(s))
Weapons Research Establishment	

12 RELEASE LIMITATIONS (of the document):

Approved for Public Release

12.0	OVERSEAS	NO		P.R.	1	A		B		C		D		E	

Security classification of this page: UNCLASSIFIED

Security classification of this page: UNCLASSIFIED

13 ANNOUNCEMENT LIMITATIONS (of the information on these pages):

No Limitation

14 DESCRIPTORS:

a. EJC Thesaurus Terms	Aircraft noise Ground effect Elastic waves Temperature inversions
b. Non-Thesaurus Terms	Acoustic ray tracing Meteorological effects

15 COSATI CODES:

2001
0402

16 LIBRARY LOCATION CODES (for libraries listed in the distribution):

SW SR SD AACA

17 SUMMARY OR ABSTRACT:
(if this is security classified, the announcement of this report will be similarly classified)

Dickinson (J. Sound and Vib 47, 438-443, 1976) reported observations of unexpectedly low attenuations between aircraft take-off noise levels measured at ranges of 320 m and 2900 m at London (Gatwick) Airport. The anomalous attenuations were attributed to the effects of focussing by a temperature inversion. These data are investigated and a ray trace study shows that the low attenuations are unlikely to be caused by atmospheric focussing by the temperature inversion. Further, it is shown that a combination of the effects of a finite impedance ground and of atmospheric refraction in overcoming part of the ground absorption at the distant position can adequately explain the observed data.

TABLE OF CONTENTS

LIST OF TABLES

LIST OF FIGURES

4. Sketch plan of Horley-Gatwick area showing location of focussing region for the measured meteorological conditions. M1, M2 are the noise measuring positions used in reference 1

5. Source-receiver geometry for straight line propagation

6. Assumed free-space 1/3 octave band levels for source at a distance of 320 m

7. Comparison between model predictions and excess attenuations measured by Parkin and Scholes(ref.10) for a range of 347 m. The model parameter is 1.5×10^5 MKS units. Data is taken from reference 4

8. Model excess attenuations for source-receiver geometry of reference 1 and various values of the model parameter ($\times 10^5$ MKS units). Range is 320 m

9. Predicted noise level at closer measuring position (R = 320 m) as a function of the model parameter when ground attenuation included

10. Diagram showing grouping of rays according to maximum height reached; (a) Ray Group 1 with initial elevation angle θ_1, (b) Ray Group 2 with initial elevation angle θ_2. Note vertical scale exaggerated

11. Diagram illustrating composite source or receiver and path difference calculation

12. Predicted noise levels for first four ray groups as a function of initial angle of elevation θ. Values are for source-receiver geometry of reference 1 and the model parameter is 1.0×10^5 MKS units. Atmospheric absorption and spherical spreading attenuation included

13. Frequency distribution of the observed attenuations between the two microphone positions. Aircraft types for each attenuation range are also shown

1. INTRODUCTION

Noise propagation over the earth's surface is strongly influenced by meteorological conditions and by the presence of the ground surface itself. These influences are particularly strong when both the source and receiver are located near the ground and for any particular case it is often difficult to separate their relative contributions to observed sound attenuations. Dickinson(ref.1) has reported observations of aircraft take-off noise levels measured at two locations (ranges 320 m and 2900 m) from the east-west runway at London (Gatwick) Airport. Unexpectedly low attenuations between the two measuring positions were observed and were attributed to the presence of a strong elevated temperature inversion which was observed concurrently by radiosonde ascent.

The purpose of this paper is firstly to show, using ray tracing, that focussing of sound waves by the temperature inverstion would not be expected to influence the observations and secondly, to propose an alternative explanation for the observations which depends upon the presence of a reflecting ground plane. The derived sound levels using this model will be shown to be in good agreement with the observations. In Section 2 the measurements reported in reference 1 are briefly summarised and in Section 3 a study of the expected influence of the temperature inversion is made using ray tracing techniques. The effect of a finite impedance ground is considered in Section 4 and expected acoustic attenuations are derived using this model and compared with the observations. The implications of these results are discussed in Section 5.

2. SUMMARY OF OBSERVATIONS

The observations reported in reference 1 were made at two measuring positions at ranges of 320 m and 2900 m north of the east-west runway at London (Gatwick) Airport on 18 December, 1971. These positions were chosen to investigate noise levels representative of those at Horley, a small town on the north-eastern flank of the airport where unusually high noise levels had been reported. The microphones were mounted at a height of 1.2 m above essentially level ground covered with thick short grass. The useful data reported are all of aircraft taking-off to the west, both measuring positions and the start-of-roll position being in line and at right angles to the direction of take-off. The noise event used to measure the attenuation between the two measuring positions was the peak level that occurred as the pilot opened the throttle and released the brakes at the commencement of take-off. The noise level observations are summarised in Table 1 (taken from Table 3 of reference 1). Nineteen events in all are reported, the attenuation between the two sites ranging between 3 and 31 dB with a mean value of 14 dB (noise levels measured in dBA). The noise level difference due to spherical spreading and atmospheric absorption was expected by Dickinson to be approximately 24 dB and the lower observed difference was attributed to the effects of the temperature inverstion which was observed to be present during the measurement period. The temperature and wind profiles obtained from the 1200 GMT radiosonde ascent at Crawley, several kilometres to the south of the airport, are shown in figure 1 (data from reference 1). A strong elevated temperature inversion was observed in the height range 280 to 490 m. This inversion apparently persisted for some time and may be a subsidence inversion associated with the trailing edge of a high pressure region centred over Central Europe which had remained virtually stationary for about seven days prior to 18 December, 1971 (ref.2). The surface weather observations made during the measurement period indicate that conditions were stable, with light breezes of 1 m/s (direction 255^{o}), a temperature of 9^{o}C and 90% relative humidity being recorded at both 1635 hours and 1952 hours. As the measured attenuations were generally substantially smaller than those expected (a difference of between +7 and -21 dB, mean 10 dB), Dickinson concluded that these data were consistent with the view that temperature inversions can cause intensification of noise levels by up to 15 to 20 dB.

3. RAY TRACING STUDY

An investigation of acoustic propagation under the meteorological conditions prevailing during the noise measurements was undertaken by ray tracing using methods developed in reference 3. Cubic spline interpolation was used between the observed data points of both the temperature and wind profiles of figure 1. The calculated range-θ diagram is shown in figure 2 for propagation to the north ($\varphi = 0$), the angle θ being the initial elevation angle of the ray from the horizontal. A source height of 2.5 m and a receiver height of 1.2 m have been used in the ray trace calculations, the results being only weakly dependent on small changes in these parameters however. The sharp changes in gradient of the range-θ curve at ranges near 7 km are due to the temperature inversion The resulting plot of intensity versus range is shown in figure 3 for an assumed source noise level of 110 dB at 100 m. The intensities in figure 3 have been calculated using constant energy flux in ray tubes and, in the region where multiple direct ray arrivals occur, incoherent energy summation has been assumed. Atmospheric absorption has not been included and the effects of multi-hop rays which suffer one or more ground reflections between source and receiver have also not been considered.

The intensity variation is close to that for spherical spreading out to ranges near 6.5 km where the effects of the temperature inversion are first observed. The inversion causes focussing of acoustic energy which gives rise to increased intensities in a small region approximately 500 m wide and centred on 6.8 km. The increase in intensity over spherical spreading is of the order of 10 dB. Note that ray theory predicts infinite intensities at the edges of this region and a full wave solution is required to determine the intensities at these points. At greater ranges the intensity falls off at a faster rate than that for spherical spreading. The intensities in the focussing region are of the right order to explain the observations reported by Dickinson, however the predicted range is over twice that of the far measurement position.

The calculations were repeated for a range of azimuth angles all to the north of the airport. The boundaries of the focussing region in which intensities above spherical spreading are to be expected have been plotted on an approximate area plan in figure 4. The width of the region increases in both directions from north while the predicted intensity within the region decreases. For example, at azimuths of $\varphi = \pm 40^{\circ}$, the intensity excess over spherical spreading has fallen to approximately 5 dB. The focussing region in figure 4 lies well beyond Horley and at approximately twice the range of the further measurement position. It would therefore be expected that focussing by the temperature inversion is not the cause of the observed low attenuations between ranges of 320 m and 2900 m.

The temperature and wind data used for the ray tracing were obtained by a radiosonde flight at 1200 GMT, some three hours before the commencement of the noise measurements. The surface conditions were virtually unchanged from 1200 GMT up to the end of measurement programme indicating stable conditions, however if the inversion layer descended during this period the range to the focussing region would be expected to be reduced, perhaps sufficiently to encompass the far measuring position. In order to investigate this possibility the inversion height was artificially reduced by 100 m as shown by the dashed profiles in figure 1. The height of the top of the strong wind shear layer was also reduced by 100 m as it is probably related to the inversion height. A new set of ray paths were calculated for these modified conditions for propagation to the north and the new range-θ curve is shown in figure 2 (dashed curve). The zero gradient portions of the original curve which correspond to infinite intensity (ray theory) have been removed. The intensity increase over spherical spreading has been reduced to approximately 4 dB (see dashed curve of figure 3) at a reduced range centred at 4 km. Thus a modification to the observed meteorological data of this order is not sufficient to explain the observed increased intensities at a range of 2900 m. Many other changes to the meteorological data are of course possible, some of which may predict intensification at the desired range. However the stability of the surface data and the

fact that the reduced attenuation between the measuring positions is seen to persist for a period of at least six hours (Table 1) suggests that the meteorological conditions are particularly stable and that the measured profiles of figure 1 are probably representative of conditions during the measurement programme.

4. PROPAGATION OVER FINITE IMPEDANCE GROUND

4.1 Surface model

The principal effect of the presence of a ground plane between source and receiver is to introduce the possibility of more than one propagation path. In the simplest case of downwind propagation over short distances the acoustic pressure at the receiver will have contributions from both the direct wave and the surface reflected wave (figure 5). Here the effect of atmospheric refraction has been assumed to be negligible. For longer ranges where refraction must be taken into account, many paths become possible. These are considered in detail below. Even in the simplest case, a knowledge of the complex acoustic impedance of the ground surface is required in order to estimate the sound pressure at the receiver. The development of the surface model to be used here is described in detail in reference 4. The acoustic properties of fibrous absorbent materials are used to model the impedance of real soil surfaces. This model was originally suggested by Delany and Bazley(ref.5). These authors measured the acoustic properties of a wide range of fibrous absorbent materials. The measured values of characteristic impedance and propagation coefficient were shown to normalise as a function of frequency (f) divided by specific flow resistance per unit thickness (σ) and to be able to be represented by simple power law functions. Expressing the characteristic impedance Z of the material as

$$Z = R + i X \tag{1}$$

the experimentally determined power law relations are as follows:

$$R/\rho_o c_o = 1 + 9.08(f/\sigma)^{-0.75} \tag{2}$$

$$X/\rho_o c_o = -11.9(f/\sigma)^{-0.73} \tag{3}$$

where c_o is the velocity of sound in air and $\rho_o c_o$ is the characteristic impedance of air. This model was used by Delany and Bazley(ref.6) to predict propagation attenuations using a plane wave reflection coefficient for the reflected wave in figure 5. Agreement with experimental data was only fair, however it has been shown in reference 4 that by considering the reflection of spherical waves from the surface, then excellent agreement with experimental measurement can be obtained for short ranges and also for ranges out to 1 km. The model was applied by choosing the value of flow resistance which gave a best fit to the experimental data in each case.

This model for the surface impedance will be used to study the effect of the presence of the ground in the experimental situation described in reference 1. The model parameter, the flow resistance σ, can be varied to study the effects of different ground surfaces.

4.2 Noise source

A knowledge of the spectral content of the noise is required for prediction of surface and atmospheric attenuation effects. The noise source used by Dickinson was the peak noise level that occurred during aircraft engine run-up prior to take-off. A variety of aircraft types were measured (Table 1), the most common type being the BAC1-11, a twin-engined turbo-fan aircraft. Noise spectra obtained at the sideline under the conditions of the experimental measurements are not available so that a typical overflight noise spectrum for a twin-engined turbo-fan aircraft measured at 305 m (1000 ft) was used. These 1/3 octave band noise levels were obtained from reference 7 and are assumed to represent the free space noise levels of the source on the sideline at the range of the closer measuring position (320 m). This assumption clearly involves some approximation, the sensitivity of the model predicted attenuations to changes in spectral shape is discussed in Section 4.5. The assumed 1/3 octave band free space noise levels of the source are shown in figure 6. A-weighted source levels are also shown (observations have been made using A-weighting as this response is close to that of the human car). The atmospheric absorption between the two measurement positions for this source is 8 dB for the measured surface conditions of a temperature of 9°C and 90% relative humidity. The expected attenuation between the measuring positions is thus 27 dB (including 19 dB spherical spreading attenuation) rather than the 24 dB assumed by Dickinson and discussed in Section 2 above.

4.3 Short range propagation

Considering the case of reflection of a plane sound wave from a normal impedance boundary in which propagation in the second medium is ignored (the case of local reaction), the expression for the plane wave reflection coefficient R_p may be written as:

$$R_p = \frac{\sin\theta - Z_1/Z_2}{\sin\theta + Z_1/Z_2} \qquad (4)$$

where Z_1 is the characteristic impedance of the first medium, taken here to be air, Z_2 is the characteristic impedance of the second medium and θ is the horizontal angle of incidence (figure 5). The simpler local reaction results of Ingard(ref.8) are used here as they have been shown to predict excess attenuations which are almost identical to attenuations obtained when propagation in the second medium is considered for the source-receiver geometries and ground impedances of interest to outdoor sound propagation (ref.4).

The velocity potential Φ at the source in figure 5 can be approximated by

$$\Phi = \frac{\exp(ikr_1)}{r_1}\left[1 + \frac{r_1}{r_2} Q \exp(ik\Delta r)\right] \qquad (5)$$

where k is the propagation coefficient in air, r_1 and r_2 are the path lengths of the direct and reflected waves and Δr is the path length difference. The image source strength Q is given by

$$Q = R_p + F(w)(1 - R_p) \qquad (6)$$

where F(w) is the boundary loss factor and w the numerical distance given by

$$w = \frac{ikr_2}{2} \frac{(\sin\theta + Z_1/Z_2)^2}{(1 + \sin\theta\ Z_1/Z_2)} \quad (7)$$

Suitable formulae for evaluating the function F(w) are given in reference 4. The excess attenuation due to the presence of a boundary over the case of free space attenuation is given by (from equation (5))

$$A_e = 20 \log_{10}|1 + \frac{r_1}{r_2} Q \exp(ik\Delta r)| \quad (8)$$

Expressing Q as $|Q|e^{i\beta}$, A_e can be written as

$$A_e = 10 \log_{10}[1 + \frac{1}{r'^2}|Q|^2 + \frac{2}{r'}|Q| \cos(\frac{2\pi\Delta r}{\lambda} + \beta)] \quad (9)$$

where $r' = r_2/r_1$. In this section comparisons of the model predictions with experimentally measured absorption losses will be made using a specified noise source averaged over 1/3 octave band levels (figure 6). The effect of finite bandwidth is dependent upon the spectrum shape but results reported in reference 9 indicate that the assumption of white noise introduces only small errors for a wide range of spectrum shapes. Equation (9) is therefore modified to the following form for averaging over 1/3 octave bands:

$$A_e = 10 \log_{10}[1 + \frac{1}{r'^2}|Q_i|^2 + \frac{2}{r'}|Q_i| \sin(\mu\Delta r/\lambda_i) \times \cos(\eta\Delta r/\lambda_i + \beta_i)/(\mu\Delta r/\lambda_i)] \quad (10)$$

where

$$\mu = 2\pi\Delta f/2f_i \quad (11(a))$$

$$\eta = 2\pi[1 + (\Delta f/2f_i)^2]^{\frac{1}{2}} \quad (11(b))$$

and the Q_i, β_i and λ_i are the values corresponding to the centre frequency of the 1/3 octave bands.

Excess attenuations predicted using equation (10) and the fibrous absorbent model for the ground impedance (equations (2) and (3)) were compared to a variety of experimentally measured excess attenuations in reference 4. Of particular importance to the situation being considered here is the comparison with jet noise measurements made by Parkin and Scholes(ref.10). The field measurements were made over essentially flat grass covered ground at eight ranges varying from 19.5 to 1097 m from a jet noise source at a height of 1.83 m using microphones mounted 1.52 m above the ground. The excess attenuation measurements were made at weekly intervals over a period of one year at times near midday and the results are confined to temperature lapse or near neutral conditions. Strong correlation was found between attenuations and the vector surface wind and the results were broken down to three cases of vector winds of +5 m/s, 0 and -5 m/s for both summer and winter. The observed excess attenuations in each 1/3 octave band in the range 50 Hz to 4 kHz are shown for four of these cases in figure 7 for a range of 347 m. This range is chosen as being similar to the closer microphone (R = 320 m) used by Dickinson. Parkin and Scholes used the observed

sound levels at the nearest microphone (R = 19.5 m) as the reference for calculating the excess attenuation. The results for a vector wind of -5 m/s are not used as they are strongly influenced by the formation of shadow zones. The excess attenuations calculated using equation (10) and the fibrous absorbent model are also shown plotted in figure 7. A model parameter of $\sigma = 1.5 \times 10^5$ MKS units was used for the calculations as this gives an overall best fit to the observed data. The model results are in good general agreement with the seasonal mean measurements, particularly for the zero vector wind cases.

This agreement between the model and excess attenuations measured at a range of 349 m supports the straight line propagation approximation assumed in equation (10) at this range and suggests that the model may be used to predict the effect of ground attenuation on the observed noise levels at the closer microphone used by Dickinson at Gatwick. The model predictions of excess attenuations compared to free space values for this source-receiver geometry are shown in figure 8 for model parameters (σ) in the range 0.5 - 4 x 10^5 MKS units. The source height has been assumed to be 2.5 m, the approximate engine height of the BAC1-11 aircraft. All curves show a deep minimum (maximum excess attenuation) in the frequency range 200 to 500 Hz. Variation with model parameter is most pronounced at low frequencies. At very low frequencies the negative excess attenuation values indicate in-phase addition of the direct and reflected waves.

The effect of this ground attenuation on the sound level at the closer measuring position is shown in figure 9 where the resulting predicted sound level is plotted as a function of model parameter σ. The assumed free space level of the source at this range of 103.6 dBa has been reduced to a level in the range 97 to 99 dBA depending upon the ground surface. The variation with surface type is small. For a model parameter of 1 x 10^5 MKS units typical of soil covered with short grass(ref.4), the received noise level is 97 dBA, a reduction over the free space level of approximately 7 dB.

4.4 Long range propagation

The effects of atmospheric refraction must be considered in any model which seeks to predict sound levels out to ranges of several kilometres from a source on or near the ground. The effects of refraction are two-fold, firstly, many more paths between source and receiver become possible and secondly, the angle of incidence at the ground for paths involving ground reflections is increased from the straight line case considered above, resulting in a decrease in ground attenuation. In order to predict the sound intensity at the receiver under these conditions it is useful to divide the possible ray paths up into groups based on the maximum height reached by each ray. Each group consists of four rays, the m^{th} member (m = 1, 2, 3, 4) of the n^{th} group (n = 1, 2, 3, ...) being designated $RG_n(m)$. The four member rays suffer n-1, n, n and n+1 ground reflections respectively. The first two ray groups are illustrated in figure 10. The first member of RG_1 (figure 10(a)) is the direct ray from source to receiver, the second member the ray that is reflected once close to the source, the third the ray that is reflected once close to the receiver and the fourth the ray that is reflected twice, once close to the source and once close to the receiver. The rays in the second group RG_2 of figure 10(b) all suffer an additional reflection near the centre of the path. Each succeeding group suffers a further additional reflection between source and receiver. As the source-receiver separation becomes small or refraction becomes less important, all these ray paths collapse into the two straight line paths of figure 5.

For source and receiver heights which are small compared with their separation, the rays in each group will have similar initial elevation angles and will travel along closely related paths and will thus be expected to exhibit some degree of coherence at the receiver. The extent of this coherence will depend upon the source and receiver heights and upon the

nature of the atmospheric turbulence. Ray tracing indicates that the height difference for the four rays of RG_1 is only 1.5 m for the geometry and meteorological conditions of reference 1. This distance is very much smaller than typical atmospheric scale sizes and the four rays might therefore be expected to be strongly coherent. This assumption will be made in determining the intensity contribution of each ray group. The contribution from each ray group will be combined by intensity summation to obtain the total noise level at the receiver.

By analogy with equation (8), the excess attenuation due to the presence of the ground for the n^{th} ray group may be written as

$$A_e = 20 \log_{10} |Q^{n-1}| . |1 + Q \exp(ik\Delta r_2) + Q \exp(ik\Delta r_3) + Q^2 \exp(ik\Delta r_4)| \quad (12)$$

where Δr_m (m = 2, 3, 4), is the path difference between the m^{th} ray, $RG_n(m)$ and the direct ray $RG_n(1)$. These path differences may be approximated by considering a composite source and receiver consisting of the source and receiver and their images in the ground plane (figure 11). Assuming the direct and reflected waves have the same elevation angle, a situation which will be closely approximated for the conditions of interest, the path differences are then given by

$$\Delta r_2 = 2h_s \text{ Sin } \theta \quad (13(a))$$

$$\Delta r_3 = 2h_R \text{ Sin } \theta \quad (13(b))$$

$$\Delta r_4 = 2h_s \text{ Sin } \theta + 2h_R \text{ Sin } \theta \quad (13(c))$$

Note that in equation (12) the distance ratio multiplying each of the last three terms has been omitted c.f. equation (8), the effect of these factors being insignificant. Equation (12) may then be expanded in terms of the modulus and phase of Q and modified to account for averaging over 1/3 octave bands in a similar manner to equation (9) and (10). The excess attenuations for the first four ray groups were calculated for a model parameter of 1×10^5 MKS units and subtracted from the 1/3 octave source noise levels. The total noise levels for each of the ray groups was then calculated and is shown plotted in figure 12 as a function of the initial elevation angle θ. These noise levels have been calculated for the source-receiver geometry appropriate to the measurements of reference 1 (h_s = 2.5 m, h_R = 1.2 m, R = 2900 m) and atmospheric attenuation has been included using attenuation values recommended in reference 11 for the measured surface meteorological conditions of temperature 9°C, relative humidity 90%. Spherical spreading attenuation has also been included.

The contribution to the total noise level of each ray group rises to a maximum around 2° to 3° initial elevation angle and falls again with increasing elevation angle, the fall being more rapid for the higher order ray groups which suffer more ground reflections. The total expected noise level is obtained by summation of the contribution from each ray group at the appropriate elevation angle. The range-θ curve of figure 2 for ray tracing using the measured meteorological conditions is approximately linear out to ranges well beyond 2900 m. The initial elevation angle required for this range is $\theta_o = 2.8°$. The four angles appropriate to the first four ray groups are therefore θ_o, $\theta_o/2$, $\theta_o/4$ and $\theta_o/8$. Summation of the appropriate levels

from figure 12 gives a total predicted noise level of 82 dBA at a range of 2900 m. The attenuation relative to the free space level at 320 m (104 dBA) can be broken down into the following contributions; +19 dB spherical spreading, +11 dB atmospheric attenuation and -8 dB ground attenuation due to the multiple propagation paths now possible. Note that the atmospheric attenuation is greater than for the simple spherical spreading model (+8 dB) due to the change in the shape of the noise spectrum after the inclusion of ground reflections. The predicted noise level of 82 dBA can now be compared to the observations of reference 1.

4.5 Comparison of results

The various model predictions of noise levels are set out in Table 2 to allow a comparison with the observed noise levels. The simple spherical spreading model in which the effect of the ground is neglected predicts a noise level equal to the assumed source level of 104 dBA at the 320 m position and a level of 77 dBA at the 2900 m position after allowing for +19 dB spherical spreading attenuation and +8 dB atmospheric attenuation. The predicted noise level difference between the two measuring sites is thus 27 dB. When ground effects are included the predicted level at 320 m is 97 dBA (from figure 9) for a model parameter of 1×10^5 MKS units and at 2900 m the predicted level is 82 dBA, a difference of 15 dB. The ground attenuation model prediction is thus in close agreement with the observed mean difference of 14 dB. Ground effects therefore provide an explanation for the unexpectedly low attenuation between the two measuring positions observed by Dickinson which does not involve focussing of energy by a temperature inversion. The model results suggest that ground reflections must be considered in any measurement programme which attempts to evaluate meteorological effects on noise propagation.

The sensitivity of the model predictions to changes in several of the experimental parameters was evaluated by recalculating the predicted noise levels at both measuring positions for various flow resistances and for various source and receiver heights. The results are summarised in Table 3. The predicted noise level differences are not particularly sensitive to changes in either source or receiver height. Some variation occurs with changes in the model flow resistance. Lower values of flow resistance (1.0 to 1.5×10^5 MKS units) were found applicable to open grassland with grass heights in the range 15 to 25 cm in reference 4 while higher values (3×10^5 MKS units) were found appropriate to closely cut lawns, however the extent of the dependence on grass covering as compared with the dependence on the nature of the underlying soil is by no means clear. The model parameter of 1×10^5 MKS units was chosen for comparison with the Gatwick results on the ground that on available evidence, it was most likely to represent the conditions of the experiment.

The dependence of the predicted noise levels on the source spectrum shape is somewhat more complex. The predicted noise level at the closer position is most dependent on changes in source spectrum level in the frequency range 1.5 to 5 kHz while the level for the distant position is most dependent on changes in the range 400 to 800 Hz. This difference is brought about by the combined effects of ground attenuation and atmospheric absorption. The dependence of the predicted noise level difference upon the source spectrum thus depends principally upon the relative changes made in these two frequency ranges. Some of the considerable variation in the observed noise level differences may be attributed to differing source spectrums for different aircraft types and operating conditions. The frequency distribution of the observed attenuations in 5 dB ranges is shown in figure 13. The aircraft types for each range are also shown in the figure. With two exceptions, the observations indicate a correlation with aircraft type. The bulk of the observations (all jet aircraft) are grouped in the 10 to 14 dB range, the two Comet observations lie below this range and the three observations of propeller aircraft lie well above this range.

The two exceptions are the single low measurement for a BAC 1-11 and the high attenuation for one of the Caravells take-offs. These large differences are difficult to explain, the most likely explanation being atmospheric turbulence effects which would be expected to cause considerable variations in the received noise levels, particularly at the distant measuring position. Data available on source noise spectra appropriate to these observations is too sparse to allow a detailed study of the effects of different aircaft types.

5. DISCUSSION

The investigation reported in this paper suggests that the unexpectedly low attenuations observed by Dickinson(ref.1) between noise levels at ranges of 320 m and 2900 m from the runway at London (Gatwick) Airport were not due to focussing by the concurrently observed temperature inversion. A consideration of the effects of reflections from a ground plane of finite impedance has shown that ground effects are sufficient to explain the apparent discrepancy between the observed mean noise level difference of 14 dB and the expected difference of 27 dB, this latter figure being obtained by considering spherical attenuation and atmospheric absorption alone. Two points should be noted as a consequence of these results. Firstly the suggestion that the temperature inversion did not play a role in the reported observations should not be taken to suggest that temperature inversions do not play a significant role in enhancing noise levels in cases of near surface propagation in general. The ray trace results presented in figure 3 for example show that considerable enhancement of noise levels can be caused by the presence of a temperature inversion. Inversions may play an important role in enhanced noise problems at Horley, the ray trace results merely indicating that on the particular day in question the range to the focussing region was too large.

Secondly, it is clear that the effect of ground reflections must be considered in predicting noise levels around a source on or near the ground. Ground effects are likely to be important when extrapolating noise source levels out to large distances for development of NEF contours. For example the noise levels predicted in Table 2 indicate that the noise level at a range of 2900 m will be underestimated by approximately 5 dB if the spherical spreading model alone is used. Ground effects can thus make a contribution of this order to the excess noise problem at Horley. These effects will be most important when predicting noise levels in communities close to the airport boundaries where propagation takes place over relatively clear ground.

REFERENCES

No.	Title	Title
1	Dickinson, P.J.	"Temperature Inversion Effects on Aircraft Noise Propagation". J. Sound Vib., 47, 438-443 (1976)
2	-	Weather Log, December 1971, Weather, 1971 (Supplement)
3	Chessell, C.I.	"Three Dimensional Acoustic Ray Tracing in an Inhomogeneous Anisotropic Atmosphere using Hamilton's Equations". J. Acoust. Soc. Amer., 53, 83-87 (1973)
4	Chessell, C.I.	"The Propagation of Noise Along a Finite Impedance Boundary". J. Acoust. Soc. Amer., 62, 825-834 (1977)
5	Delany, M.E. and Bazley, E.N.	"Acoustical Properties of Fibrous Absorbent Materials". Appl. Acoust., 3, 105-116 (1970)
6	Delany, M.E. and Bazley, E.N.	"A Note on the Effect of Ground Absorption in the Measurement of Aircraft Noise". J. Sound Vib., 16, 315-322 (1971)
7	-	U.S. Environment Protection Agency Report NT1D300-13, (1971)
8	Ingard, U.	"On the Reflection of a Spherical Sound Wave from an Infinite Plane". J. Acoust. Soc. Amer., 23, 329-335 (1951)
9	Thomas, P.	"Acoustic Interference by Reflection-Application to Sound Pressure Spectrum of Jets". NASA TT-F-14185, March (1972)
10	Parkin, P.H. and Scholes, W.E.	"The Horizontal Propagation of Sound from a Jet Engine Close to the Ground, at Radlett". J. Sound Vib., 1, 1-13 (1964)
11	-	"Standard Values of Atmospheric Absorption as a Function of Temperature and Humidity for use in Evaluating Aircraft Flyover Noise". Soc. of Autom. Eng. Inc., Aerospace Recommended Practice 866, 31 August (1964)

TABLE 1. MEASUREMENTS OF AIRCRAFT TAKE-OFF NOISE MADE AT LONDON (GATWICK) AIRPORT AS REPORTED IN REFERENCE 1

Time	Aircraft type	Peak noise level 320 m (dBA)	Peak noise level 2900 m (dBA)	Attenuation (dB)
1524	Caravelle	90	77	13
1533	Caravelle	95	64	31
1545	BAC1-11	96	84	12
1548	BAC1-11	98	85	13
1628	DC-6	96	75	21
1728	DC-6	90	68	22
1739	BAC1-11	96	85	11
1808	BAC1-11	91	81	10
1825	707	94	76	18
1829	707	96	83	13
1837	Viscount	95	75	20
1840	BAC1-11	90	87	3
1842	BAC1-11	97	85	12
1857	Comet	93	85	8
1928	Comet	92	89	3
1930	VC-10	101	88	13
2059	BAC1-11	96	83	13
2100	VC-10	99	85	14
2115	BAC1-11	100	89	11
				Mean 14 dB

TABLE 2. SUMMARY OF MODEL PREDICTIONS OF NOISE LEVELS AT 320 M AND 2900 M AND COMPARISON WITH MEASURED VALUES. ALL NOISE LEVELS ARE IN dBA

	Assumed source noise level (Free Space-320 m)	320 m noise level	2900 m noise level				Noise level difference (2900-320 m)
			Spherical spreading attenuation	Atmospheric attenuation	Ground Attenuation	Resultant noise level	
Spherical Spreading Model	104	104	+19	+ 8	-	77	27
Ground Attenuation Model (σ = 1.0 x 10^5 MKS units)	104	97	+19	+11	- 8	82	15
Observed (Mean)		95				81	14

TABLE 3. SENSITIVITY ANALYSIS OF PREDICTED NOISE LEVELS AND NOISE LEVEL DIFFERENCE (2900 m - 320 m) TO VARIATIONS IN THE MODEL PARAMETER, SOURCE HEIGHT AND RECEIVER HEIGHT

Source height (m)	Receiver height (m)	Model parameter ($x10^5$ MKS units)	Predicted noise level		
			320 m (dBA)	2900 m (dBA)	Difference (dB)
2.5	1.2	0.5	97	83	14
2.5	1.2	1.0	97	82	15
2.5	1.2	1.5	97	81	16
2.5	1.2	2.0	98	80	18
2.5	1.2	3.0	98	79	19
2.5	1.2	4.0	98	79	19
1.5	1.2	1.0	94	81	13
2.5	1.2	1.0	97	82	15
3.5	1.2	1.0	99	82	17
2.5	0.7	1.0	94	79	15
2.5	1.2	1.0	97	82	15
2.5	1.7	1.0	100	84	16

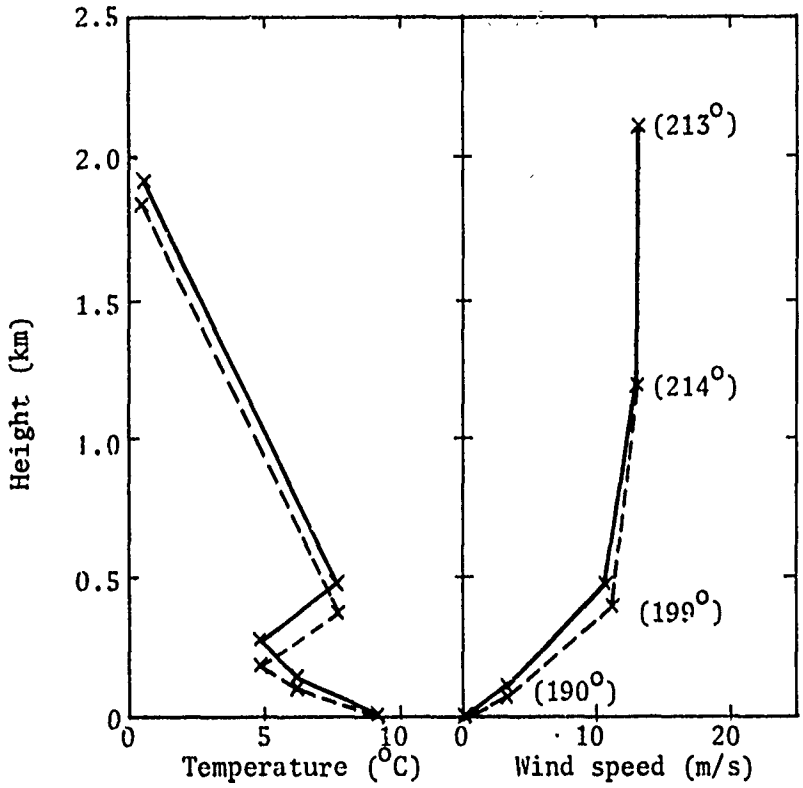

Figure 1. Temperature and wind profiles measured by radiosonde ascent at Crawley, 1200 hours GMT, 18 December, 1971 (full lines), as taken from reference 1. Dashed lines are modified profiles assuming inversion height decreases by 100 m (see text). Wind direction at each level is shown in brackets

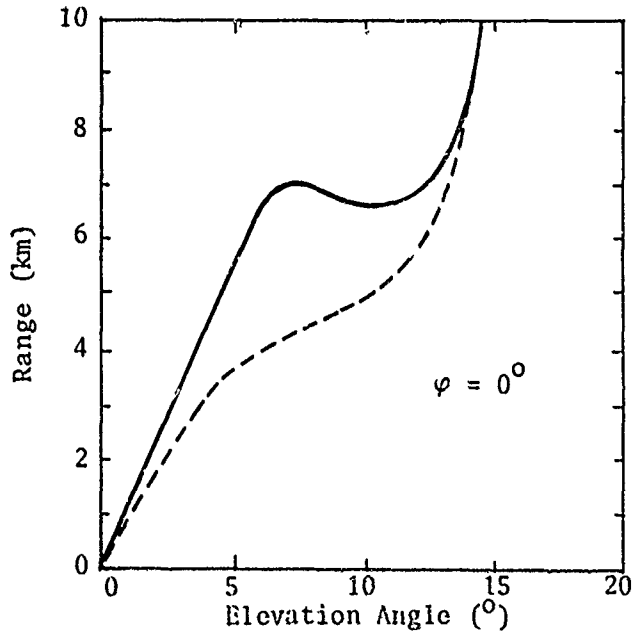

Figure 2. Range-θ diagram for measured meteorological conditions and propagation to the north (full curve). Range-θ relation for modified meteorological conditions of figure 1 is shown as broken curve

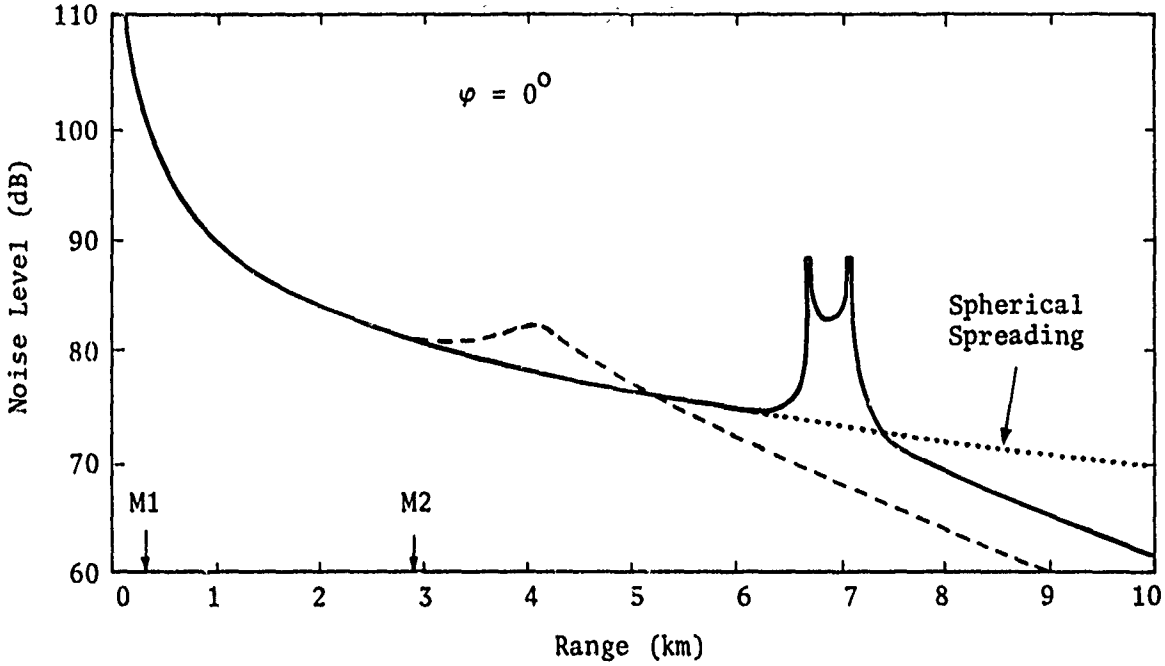

Figure 3. Range versus intensity curve for measured meteorological conditions and propagation to the north (full curve). Source level of 110 dB at 100 m assumed and single hop propagation only considered. Atmospheric absorption not included. Intensity curve for modified meteorological profile of figure 1 is shown as dashed curve

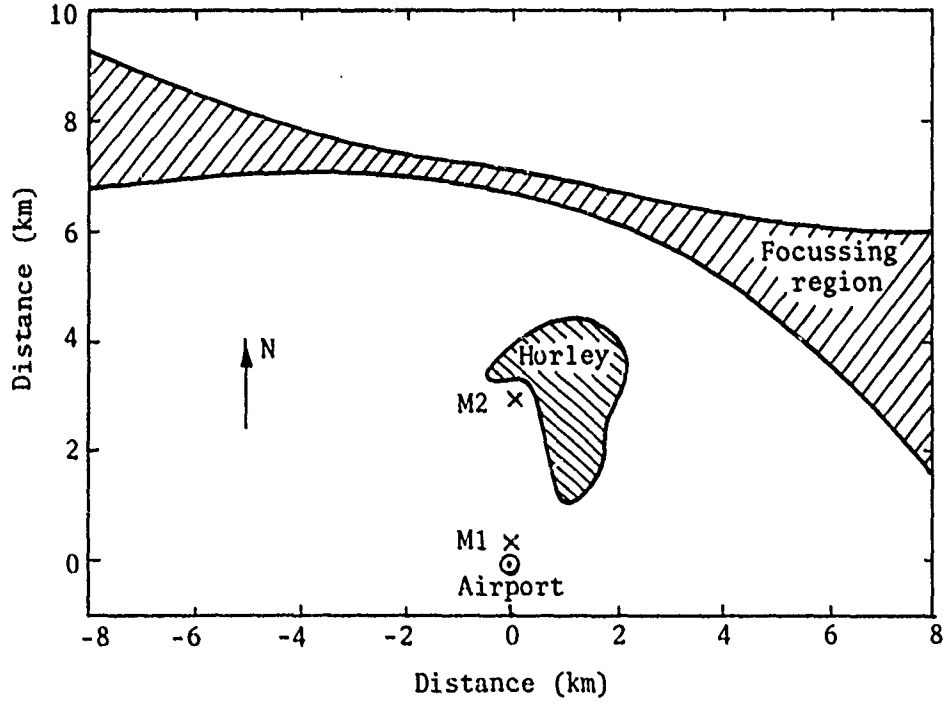

Figure 4. Sketch plan of Horley-Gatwick area showing location of focussing region for the measured meteorological conditions. M1, M2 are the noise measuring positions used in reference 1

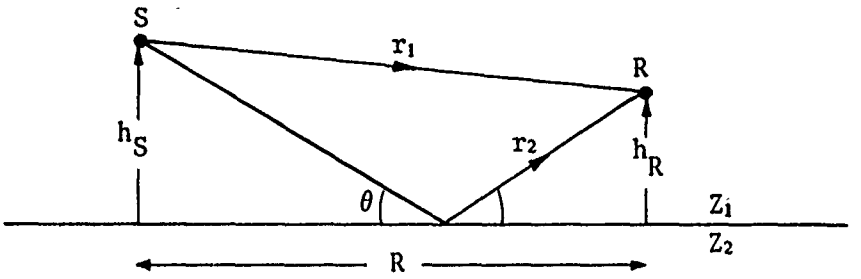

Figure 5. Source-receiver geometry for straight line propagation

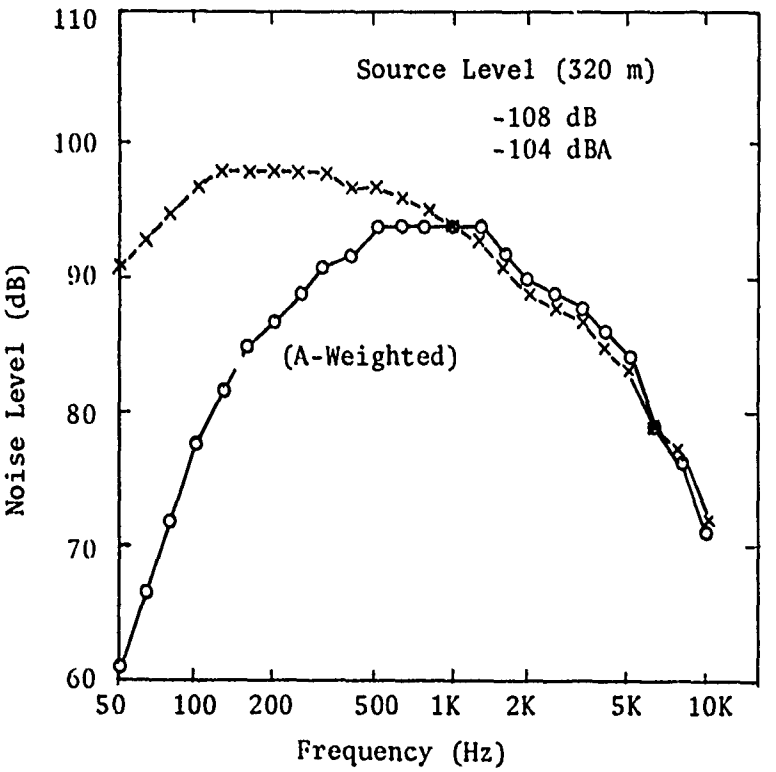

Figure 6. Assumed free-space 1/3 octave band levels for source at a distance of 320 m

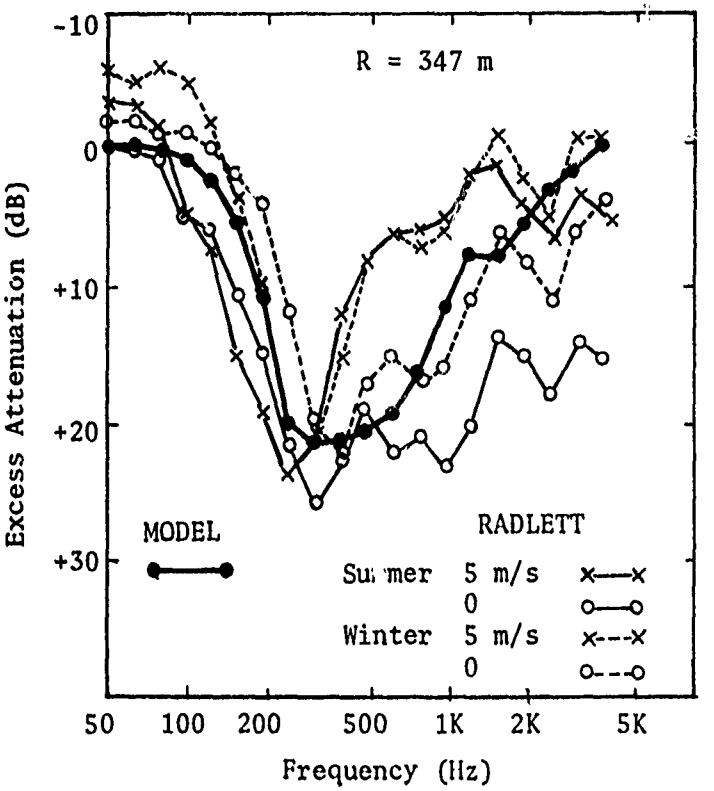

Figure 7. Comparison between model predictions and excess attenuations measured by Parkin and Scholes(ref.10) for a range of 347 m. The model parameter is 1.5 x 10^5 MKS units. Data is taken from reference 4

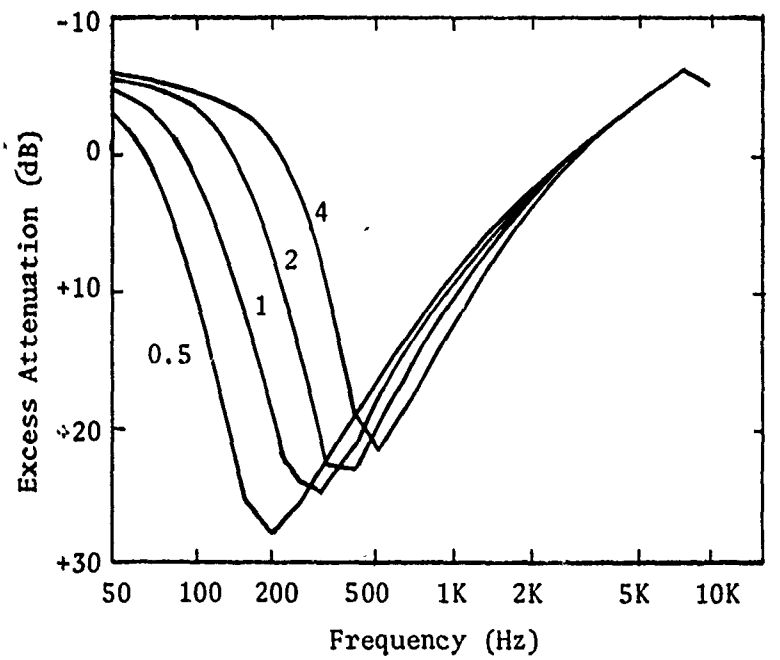

Figure 8. Model excess attenuations for source-receiver geometry of reference 1 and various values of the model parameter (x 10^5 MKS units). Range is 320 m

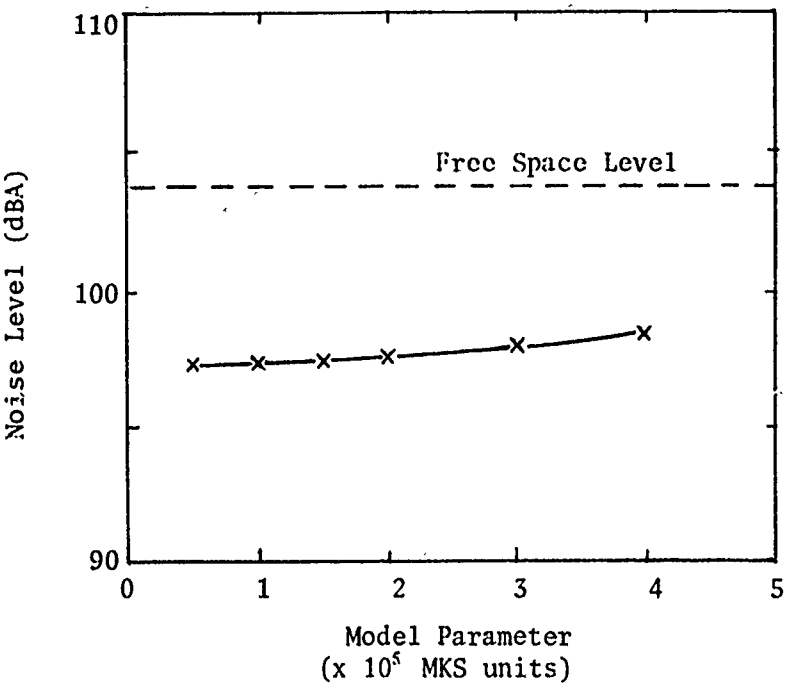

Figure 9. Predicted noise level at closer measuring position (R = 320 m) as a function of the model parameter when ground attenuation included

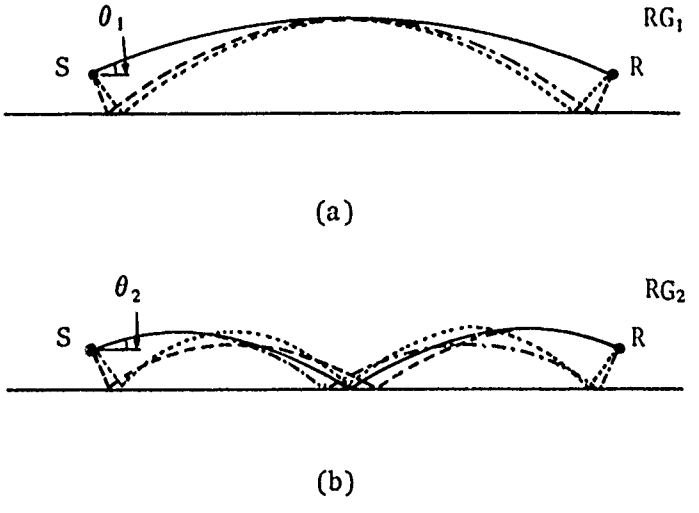

Figure 10. Diagram showing grouping of rays according to maximum height reached; (a) Ray Group 1 with initial elevation angle θ_1, (b) Ray Group 2 with initial elevation angle θ_2. Note vertical scale exaggerated

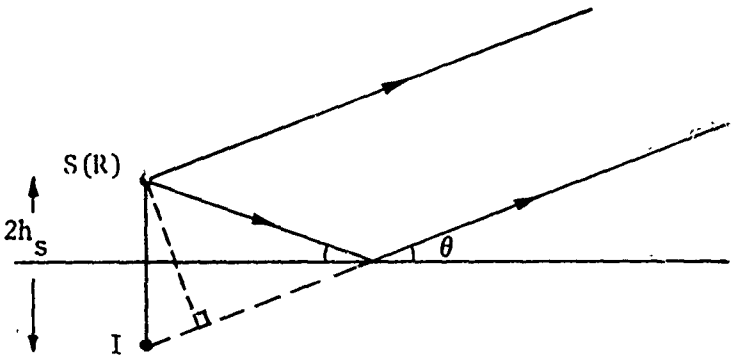

Figure 11. Diagram illustrating composite source or receiver and path difference calculation

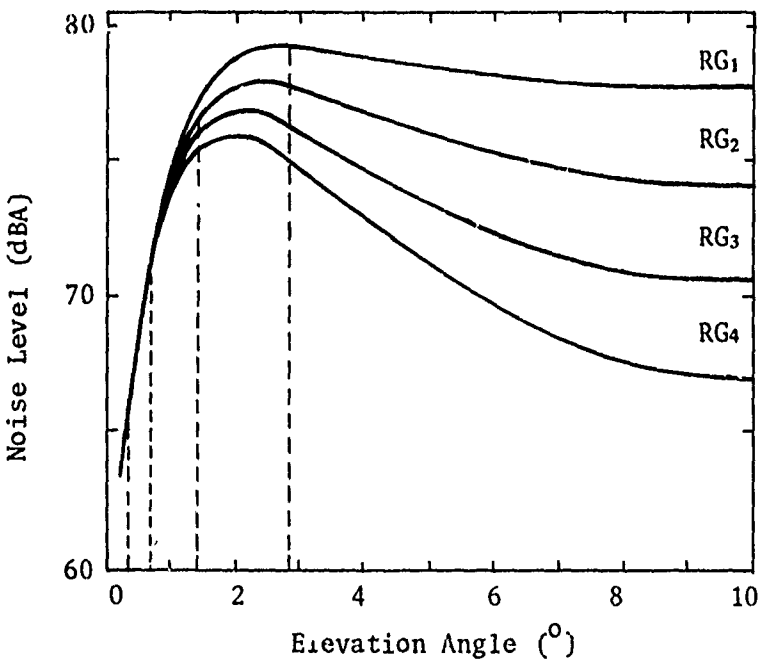

Figure 12. Predicted noise levels for first four ray groups as a function of initial angle of elevation θ. Values are for source-receiver geometry of reference 1 and the model parameter is 1.0×10^5 MKS units. Atmospheric absorption and spherical spreading attenuation included

DISTRIBUTION

EXTERNAL	Copy No.
In United Kingdom	
Defence Scientific and Technical Representative, Australia House, London	1
Institute of Sound and Vibration Research, University of Southampton	
(Attention: Professor J.B. Large)	2
(Attention: Dr P.J. Dickinson)	3
In United States of America	
Counsellor, Defence Science, Washington D.C.	4
Office of Environmental Quality, Federal Aviation Administration, Washington D.C.	
(Attention: Dr J.O. Powers)	5
National Aeronautics and Space Administration, Langley Research Centre, Hampton, Virginia, 23665	
(Attention: Dr R. DeLoach)	6
In Canada	
Acoustics Section, Division of Physics, National Research Council, Ottawa	
(Attention: Mr J.E. Piercy)	7
In Australia	
Department of Defence	
Chief Defence Scientist	8
Controller, Military Studies and Operational Analysis Division	9
Superintendent, Military Advisers Branch	10
Air Force Scientific Adviser	11
Navy Scientific Adviser	12
Army Scientific Adviser	13
Executive Controller, Australian Defence Scientific Service	14
Superintendent, Defence Science Administration Division	15
Defence Information Services Branch (for microfilming)	16
Defence Information Services Branch for:	
United Kingdom, Ministry of Defence, Defence Research Information Centre (DRIC)	17
United States, Department of Defense, Defense Documentation Center	18 - 29
Canada, Department of National Defence, Defence Science Information Service	30
New Zealand, Department of Defence	31
Australian National Library	32

	Copy No.
Defence Library, Campbell Park	33
Library, Aeronautical Research Laboratories	34
Library, Materials Research Laboratories	35
Director, Joint Intelligence Organisation (DDSTI)	36
Department of Transport	
First Assistant Secretary, Airways Operations	37
(Attention: Mr M.D. Dunne)	38
(Attention: Mr B.G. Harris)	39
Senior Assistant Secretary, Research and Development	
(Attention: Mr R.C. Lam)	40
Department of Health	
Director, National Acoustic Laboratories	
(Attention: Mr J.A. Rose)	41
INTERNAL	
Director	42
Chief Superintendent, Applied Physics Wing	43
Chief Superintendent, Weapons Research and Development Wing	44
Superintendent, Systems Analysis Division	45
Principal Officer, Tropospheric Studies Group	46
Principal Officer, Ionospheric Studies Group	47
Mr A.R. Mahoney, Tropospheric Studies Group	48
Dr P.W. Baker, Tropospheric Studies Group	49
Mr T.N. Tresidder, Tropospheric Studies Group	50
Mr Z.R. Jeffrey, Tropospheric Studies Group	51
Mr P. Rugless, Computing Services Group	52
Dr C.I. Chessell, Tropospheric Studies Group	53
Group Clerk, Tropospheric Studies Group	54 - 57
W.R.E. Library	58 - 59
Spares	60 - 67